A MIXTURE MODEL FOR FOAMY OIL FLOW IN POROUS MEDIA

D. D. JOSEPH[1], P.H. HAMMOND[2], A.M. KAMP[3], M. RIVERO[3], M. HUERTA[3]

[1]Univ. of Minnesota, Dept. of Aerospace Engng. & Mech., 107 Akerman Hall
110 Union Street. S.E., Minneapolis, MN 55455, USA

[2]Schlumberger Cambridge Research, High Cross, Madingley Road, Cambridge, CB3 0EL, England

[3]Intevep S.A., PO Box 76343, Caracas 1070-A, Venezuela

Working document

Revision 2, November 9, 1997

Abstract

The processes of nucleation, bubble growth and finally the creation of connected gas during the pressure draw-down in an oil reservoir are discussed. From these mechanisms, possible descriptions of foamy oil production appear. One of these mechanisms is the creation of bubbles, small compared to pore sizes, which move with the oil phase and which push the oil out of the reservoir. If this mechanism occurs, a very simple model can describe the production of foamy oil. This model is obtained by establishing an equilibrium relation between gas fraction and pressure, which then is modified into a constitutive equation relating gas fraction and pressure in a dynamic context where super-saturation is present. Together with a mixture mass conservation equation and Darcy's law, a two equation description of foamy oil production is obtained, depending on only two dimensionless numbers. It is thought that this is the most simple possible way to describe some particular cases of anomalous behavior of foamy oil. [Mention results]. The implications of the model for the production of foamy oil reservoirs are eventually discussed.

1 Introduction

Some heavy oil reservoirs, most of which are located in Canada and Venezuela, produce at the well-head an oil with obvious foaminess, so called foamy oil. Comparing its production to conventional solution gas drive, most of these reservoirs exhibit anomalous *high production rates* and *high primary recovery factors*. The *gas-oil ratio* is often low, and stays low in time, whereas light oil reservoirs show a rapidly increasing gas-oil ratio when the pressure decreases below the bubble point pressure (Maini, 1996). Some of the foamy oil reservoirs show anomalous high sand production and so-called worm holing (Wang, 1997, Geilikman et al., 1995, Smith, 1986) although this does not seem to be a general rule. Especially in Venezuela such anomalous sand production is rarely observed in reservoirs producing foamy oil. The solubility of gas in foamy oils does however not appear to be much higher than that in light oils (comparison of for example the Methane / Decane system with Methane / Athabasca bitumen, the solubility in the latter is found to be approximately 1.5 times higher, see Reamer et al, 1942 and Svrcek & Mehrotra, 1982).

Although the reasons for the favorable response of foamy oils in solution gas drive are not completely understood and tentative explanations which have been put forward are somewhat controversial (see Maini, 1996 and Pooladi-Darvish & Firoozabadi, 1997 for recent reviews), some general concepts of foamy oils have emerged.

Oils contain components of low molecular weight, which at initial reservoir pressures are dissolved in the oil. If the reservoir pressure is above the bubble point pressure, the oil is called *sub-saturated*. If the pressure in the reservoir is however drawn down, and the bubble point pressure is crossed, the light component can no longer be dissolved in the oil. The oil becomes *super-saturated* and starts to release gas by nucleation of bubbles and subsequent diffusion of gas into these bubbles.

Initially the bubbles are small compared to the average pore size. It is then probable that most of the bubbles move with the liquid phase, although some bubble trapping potentially might occur. The bubble sizes however gradually increase due to diffusion of gas into the bubbles and due to coalescence of several bubbles into larger bubbles. Eventually, the bubble diameter will become of the order of magnitude of average pore size. It is quite possible that if this happens, the gas and liquid can no longer be treated as a mixture and the bubbles move at a velocity which differs from the liquid velocity, because of the different relative permeability. Finally recombination of many large bubble might lead to connected gas which flows, due to its low viscosity, much more rapidly than the liquid phase. The gas fraction at which this happens is called the *critical gas saturation*. Once connected gas is created, the oil reservoir stops producing oil without artificial stimulation.

This explains the tight connection between critical gas saturation and primary recovery. When the gas becomes connected, the end of primary recovery becomes in sight. The (critical) gas saturation is then approximately equal to the fraction of oil pushed out of the reservoir, which is the primary recovery.

The distinct phases in the process of nucleation and bubble growth are schematically depicted in figure 1.

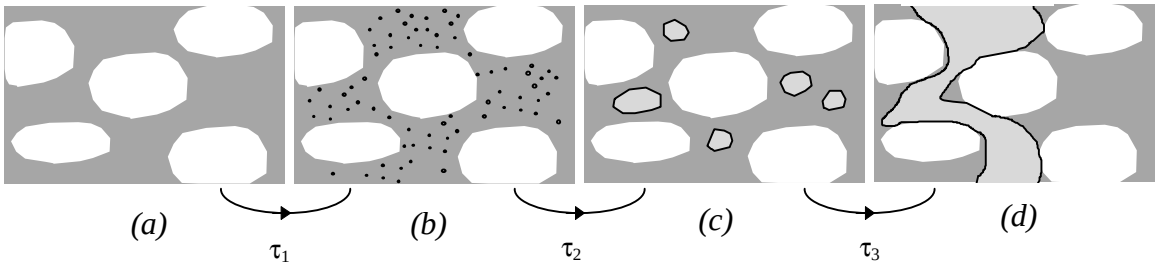

Figure 1 Schematic representation of nucleation and bubble growth in a porous media (white is rock, dark gray is oil and light gray is gas): (a) only dissolved gas; (b) bubbles small compared to average pore size; (c) bubbles of size comparable to average pore size; (d) fully connected gas. Typical time scales of transformation between the stages are indicated as τ_1, τ_2 *and* τ_3.

It is thought that the precedent description applies to any oil reservoir, whether the oil is light or heavy and independent of composition. The difference between foamy and conventional oil reservoirs is however that the characteristic time scales at which the processes occur are very different. In normal light oil reservoirs it is thought that the transformation of small bubbles, through larger bubbles to connected gas, happens on a time scale which is short compared to a characteristic time scale of the pressure draw-down of the reservoir. In foamy oils however, this is probably not the case. Possible reasons are the following

1. The viscosity of heavy oil is much higher than the viscosity of light oil and the diffusion coefficients of dissolved gas molecules are much smaller. This means that if the pressure is decreased, the transfer of gas from a dissolved state into a small bubbles occurs slower in a heavy oil than in a light oil. Therefore super saturation might at a same pressure decline be higher in heavy oil.
2. The transformation of small bubbles into large bubbles is governed by the coalescence between two bubbles, which increases the mean bubble size. The coalescence process involves the drainage of an oil film which is created between two bubbles which are in near contact. This drainage takes more time when the viscosity of the oil is higher (Chesters, 1991).
3. Also the presence of surface active components such as, for example, asphaltenes or other large chain molecules, might significantly increase drainage time by the so-called *Marangoni* effect.
4. The coalescence of bubbles is however not only governed by a film drainage process but also by a collision process which has to occur before film drainage can take place. It might be expected that the collision rate between bubbles is lower when the viscosity of the fluid is higher.

Thus the transformation of small bubbles into large bubbles and of large bubbles into connected gas, will be slower in heavy oils than in light oils.

Within this framework, some of the typical foamy oil observations can be explained. The low gas-oil ratio follows from the fact that the creation of connected gas is very slow, so that gas moves with the oil, or even slower than the oil if some bubbles are trapped. The high critical gas saturation is simply explained by the fact that coalescence between

bubbles is more difficult in a heavy than in a light oil, so that higher gas fraction can be achieved without creating connected gas. The high production rates might be directly the result of the fact that all the dissolved gas helps to push the oil out, and that none of this gas escapes the reservoir by creating channels of connected gas.

The terminology “foamy oil” might however be somewhat misleading. At actual reservoir pressures, gas fraction can be as low as 5 to 10%, far below the gas fraction value of 70% at which bubbles are arranged in close packed arrays, something usually associated with the onset of foaming. It might be possible that this bubbly liquid, that we call foamy oil, actually behaves like a foam, when bubble sizes become large. In this case, the thickness of the “oil lamellae” between the bubbles would be small compared to the bubble sizes, which might be seen as a typical characteristic of foam.

It is also not quite clear from the previous description whether foamy oils display a foaming threshold. That is to say, whether for example the rate of pressure draw-down is determining for whether the oil “foams” or not. Eventually bubbles will always be generated, but it might be that the actual bubble size depends on the pressure decline by for example differences in achieved super saturating. This change in bubble size might then influence the critical gas saturation and so couple back on achievable primary production.

1.1 A model for bubbly oils

The creation of a model for the processes of nucleation and bubble growth assumes that we know at which rates they take place. A detailed mathematical description appears however to be extremely difficult. Nucleation modeling involves often quite a lot of undetermined parameters, which are difficult to obtain in practically relevant situations. Activation energies are not well known and neither are the role and distribution of nucleation sites. Nucleation modeling often introduces extra time scales which make reservoir simulation numerically more difficult to achieve. Film drainage and coalescence between bubbles are processes on which still much work has to be done. Also the dependence of relative permeabilities on bubble sizes and gas fraction are not fully understood.

For these reasons, it seems wise to restrict potential models to the description of situations where one transfer rate is much slower than all other transfer rates. Three possibilities are indicated in table 1.

determining time scale	*observed behavior*
τ_1	few bubbles, oil heavily supersaturated
τ_2	small bubbles (possibly moving with the oil)
τ_3	large (possibly trapped) bubbles

Table 1 Different observed behaviors for different determinant time constants

In this document we will try to set up a simple description for the case where the transfer rate from bubbles to connected gas is much lower than the transfer rate for dissolved gas to bubbles.

The proposed model does not require any microscale information about nucleation, bubble growth, compressibility or forces which produce relative velocity. We put up a mixture theory in which the dispersed gas is described by a gas fraction field in a single

fluid in which the viscosity, density and mobility in Darcy's law all depend on the gas fraction. This fluid satisfies the usual Darcy law, and the continuity equation together with a kinetic (constitutive) equation required by the condensation and outgassing of the heavy crude. The theory depends only on three parameters which can be measured in a PVT cell and sand pack experiments: a mobility, a solubility and a time constant for mass transfer from a dissolved state to free gas. The virtue of the model is simplicity, but it can only work if the gas is dispersed and moves with the oil. If the gas phase does not move with the oil, no relation between local concentration of dissolved gas and local gas fraction can be derived.

Certainly the theory could not be expected to give rise to a percolation threshold or even to a critical gas fraction, but it might describe many features of solution gas drive of foamy oils in the dispersed bubbly mixture regime.

It is our idea that the increased recovery and production are generated by the pumping of nucleating and growing gas bubbles. The gas fraction increases the volume of the composite fluid and it acts as a pump, the gas coming out of solution pumping the fluid outward. This pumping action is well described by the continuity equation (2.24) which implies that in a closed volume V with boundary S containing dispersed bubbles of gas fraction ϕ.

$$\int_V \frac{1}{1-\phi}\frac{D\phi}{Dt}dV = \oint_S \mathbf{u}_m \cdot \mathbf{n} dS \tag{1.1}$$

Where $\mathbf{n}$ is the outward normal on S and $\mathbf{u}_m$ is the velocity of our composite fluid.

2 Model description

2.1 Solubility of gas in crude oil

In this model we avoid all constitutive equations regarding nucleation rates, bubble growth, and compressibility. In our model we have only foamy oil and dispersed gas, but the dispersed gas enters only through

$$\phi = \frac{V_g}{V_l + V_g} \tag{2.1}$$

where V_g is a volume of dispersed gas and V_l is the volume of liquid.

We propose to describe the evolution of ϕ by a linear kinetics evolution equation for uniform samples in a PVT cell of the form

$$\gamma\tau_1 \frac{D\phi}{Dt} + \tau_2 \frac{Dp}{Dt} = f(\phi, p) \tag{2.2}$$

where τ_1 and τ_2 are characteristic time scales and γ is a constant with dimension pressure. $f(\phi, p)$ is a function which is to be determined from experiments.

The derivatives in (2.2) are material derivatives defined by

$$\frac{D}{Dt} = \alpha\frac{\partial}{\partial t} + \mathbf{u}_m.\nabla \tag{2.3}$$

where α is the porosity of the medium and $\mathbf{u}_m$ the superficial velocity of mixture flow in the porous medium.

We have equilibrium whenever

$$f(\phi, p) = 0 \tag{2.4}$$

Svrcek and Mehrotra (1982) give volumetric solubility curves (CO_2 and methane CH_4, in figure 2.1). In these figures $\hat{V}$ is the ratio between the volume of gas that can be evolved out of bitumen when the pressure is dropped to less than one atmosphere at a temperature of 100°C and the original volume of bitumen. We can assume that this tells you how much dispersed gas can come out of solution of condensed gas which is at a saturation value at any pressure and temperature. We are going to assume that this $\hat{V}$ determines the dispersed gas fraction ϕ following an argument put forward in what is to follow.

[insert solubility graphs from Svrcek & Mehrotra]

Figure 2.1 Svrcek & Mehrotra (1982) solubility curves $\hat{V}$ vs. p

In the present approach we have no way to predict the size or size distribution of gas bubbles. This means that we are free to choose the size and distribution to measure $\hat{V}$ and the most convenient choice is when all the released gas is collected at the top of a PVT such as in the experiment of Svrcek & Mehrotra. Figure 2.2 describes such a depressurization experiment

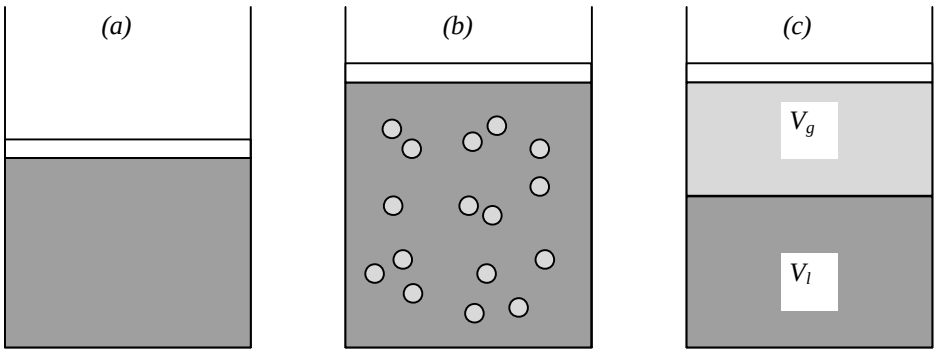

Figure 2.2 Depressurization experiment in PVT cell at constant temperature; the oil is indicated in dark gray, the gas in light gray. (a) dissolved gas at pressure p and temperature T; (b) just after the pressurization, pressure p_{ref} and temperature T_{ref}; (c) Finally all the gas percolates out and $\hat{V} = V_g / V_l$ can be measured.

The pressure in a saturated live oil is suddenly decreased from pressure p to reference pressure $p = p_{ref}$. Bubble nucleate and eventually percolate out of the oil. Svrcek & Mehrotra measure a gas-liquid ratio defined as

$$\hat{V} = \frac{V_g\left(p_{ref}\right)}{V_l(p)} \tag{2.5}$$

which is the volume of gas that comes out of solution when the pressure is dropped to a reference pressure p_{ref} and temperature T_{ref}. Their data show that

$$p - p_0 = \hat{\gamma}(T)\hat{V} \tag{2.6}$$

where $\hat{\gamma}$ is a reciprocal solubility and $p = p_0$ at $\hat{V} = 0$. This $\hat{V}$ is the solubility of the gas given as a volume ratio and it is plotted in figure 2.1. The saturated bitumen is called "live oil". $\hat{V}$ is the volume ratio of dispersed gas which comes out of solution.

We suppose that all the gas which comes out of solution is disperse and does not percolate. In the experiments in figure 2.1, we must suppose that the nucleation, growth and compressibility of gas bubbles are working, but these microstructural features are suppressed in these experiments; embedded all in the solubility $\hat{V}$. This is also what we do in the mathematical model.

We slightly alter a solubility isotherm in the cartoon of figure 2.3 below.

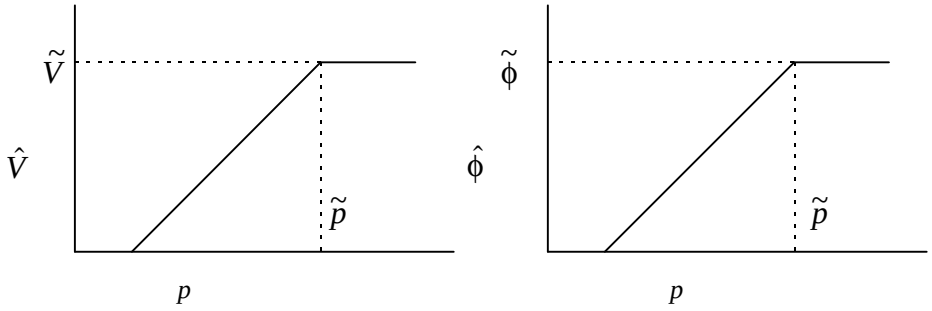

Figure 2.3 Solubility isotherm used in this model

Suppose, at some high pressure, which is called the bubble point pressure $p = \tilde{p}$, that $\hat{V} = \tilde{V}$, and that there is no more gas available to go into solution; Equation (2.6) can then be written as

$$\tilde{p} - p = \hat{\gamma}\left(\tilde{V} - \hat{V}\right) \tag{2.7}$$

If we bring back the relative volume $\hat{V}$ of gas that has come out of solution at the reference pressure and temperature to the original pressure and temperature, we obtain a relative volume of dissolved gas which we call $\hat{\phi}$

$$\hat{\phi} \equiv \frac{p_{ref}}{p}\frac{T}{T_{ref}}\hat{V} \tag{2.8}$$

And from (2.7)

$$\tilde{\phi} - \hat{\phi} = \left(\frac{p_{ref}}{\hat{\gamma}(T)}\frac{T}{T_{ref}}\right)\frac{1}{p}\left(\tilde{p} - p\right) \tag{2.9}$$

The dependence on $1 / p$ is a compressibility effect, whereas $\tilde{p} - p$ comes from gas coming out of solution. In other words, decreasing the pressure, increases the compressibility of the mixture by gas coming out of solution and by increasing the

compressibility of the free gas. The latter effect is however weak at pressure close to the bubble point pressure $\tilde{p}$. So (2.9) can be approximated by

$$\tilde{\phi} - \hat{\phi} = \frac{1}{\gamma}(\tilde{p} - p) \tag{2.10}$$

where the parameter γ

$$\gamma(T) \equiv \hat{\gamma}(T)\frac{p}{p_{ref}}\frac{T_{ref}}{T} \approx \hat{\gamma}(T)\frac{\tilde{p}}{p_{ref}}\frac{T_{ref}}{T} \tag{2.11}$$

can be considered constant. The gas is thus considered incompressible.

From volume conservation we find that the relative volume of gas that comes out of solution when the pressure is dropped from $\tilde{p}$ to p is

$$\frac{V_g}{V_l} = \tilde{\phi} - \hat{\phi} \tag{2.12}$$

If the volume of free gas stays low compared to the total volume, then

$$\phi = \frac{V_g}{V_g + V_l} \approx \frac{V_g}{V_l} \tag{2.13}$$

and combining this with (2.12)

$$\phi = \tilde{\phi} - \hat{\phi} \tag{2.14}$$

Substituting this result in (2.9) we find that gas fraction and pressure are approximately linearly related

$$\tilde{p} - p - \gamma(T)\phi = 0 \tag{2.15}$$

In the following we will call this equation the equilibrium solubility.

2.2 Dynamic constitutive equation

The equilibrium solubility relation (2.15) can be seen as a degeneration of (2.2). In this case the gas fraction and the dissolved mass fraction of gas are in instantaneous equilibrium with the pressure.

In many cases however, gas cannot come out of solution infinitely fast when pressure is changed, so that equation (2.15) has to be violated. The rate at which gas can come out of solution by nucleation of bubbles and diffusion of gas to these nucleated bubbles might be predicted by a theory of nucleation and diffusion. These theories are however complex and involve several constants which are difficult to quantify. Therefore we suggest the that the dynamic behavior of solubility be described in terms of equation (2.2). In the following we will concentrate on the special case

$$\tau\frac{Dp}{Dt} = f(p,\phi) \tag{2.16}$$

(in appendix A another special case is discussed)

Assuming linear kinetics, we propose then from (2.15) and (2.16)

$$\tau\frac{Dp}{Dt} = \tilde{p} - p - \gamma\phi \tag{2.17}$$

which is a rate equation of the Maxwell type.

$Dp/Dt = 0$ when p and ϕ are at equilibrium and satisfy (2.15). When p is below this value and ϕ at equilibrium, then $dp/dt > 0$ and the pressure will increase to its equilibrium value. When $\phi = 0$, $p - \tilde{p}$ relaxes to zero exponentially.

Including of a term proportional to $D\phi / Dt$ would lead to an Oldroyd B type of model (see also appendix A) with a retardation as well as relaxation time.

2.3 Governing equations

In addition to the constitutive equation (2.17), the flow is described by a mass conservation equation for the mixture of gas and liquid

$$\frac{D\rho_m}{Dt} + \rho_m \nabla \cdot \mathbf{u}_m = 0 \tag{2.18}$$

where ρ_m is the mixture density defined by

$$\rho_m = (1-\phi)\rho_l + \phi\rho_g \tag{2.19}$$

The mixture velocity $\mathbf{u}_m$, which is the mixture flow rate divided by the total cross sectional area of the porous medium, is supposed to be well represented by Darcy's law

$$\mathbf{u}_m = -\lambda(\phi)\nabla p \tag{2.20}$$

Here the mobility λ is the ratio between permeability κ and mixture viscosity μ_m

$$\lambda(\phi) = \frac{\kappa}{\mu_m} \tag{2.21}$$

It is not expected that the mixture viscosity μ_m is very different from the oil viscosity μ_l, because the bubbles are assumed small and the gas fraction low. Since the oil viscosity increases as the quantity of dissolved gas decreases, μ_l and thus μ_m are expected to be some increasing function of the gas fraction. Based on this argument, λ would decrease as the gas fraction increases.

If it further assumed that the gas density is small compared to the oil density $\rho_g << \rho_l$, then (2.19) can be approximated by

$$\rho_m \approx (1-\phi)\rho_l \tag{2.22}$$

After substitution of the definition of the material derivative (2.3), the mixture density (2.22) and the mixture velocity (2.20) in equation (2.17) and (2.18), we obtain

$$\alpha\frac{\partial p}{\partial t} - \lambda|\nabla p|^2 = \frac{\tilde{p} - p - \gamma\phi}{\tau} \tag{2.23}$$

$$\alpha\frac{\partial \phi}{\partial t} - \lambda\nabla p \cdot \nabla\phi = (1-\phi)\nabla\cdot(-\lambda\nabla p) \tag{2.24}$$

which are the two fundamental equations of the model.

It is possible to eliminate the gas fraction from the problem, which gives rise to a very non-linear partial differential equation in pressure.

2.4 Dimensionless analysis

In order to make numerical solution of the equations easier and to determine the number of independent constants in the problem, it is convenient to write the equations in a dimensionless form. Therefore we choose a typical length scale L and a typical pressure

difference Δp. A dimensionless time can be chosen as $t\lambda\Delta p / \alpha L^2$, a dimensionless pressure as $(\tilde{p} - p)/\Delta p$ and a dimensionless void fraction as $\gamma\phi / \Delta p$. Although the mobility might depend on bubble size and gas fraction, we suppose that these dependencies can be neglected in first order approach. Therefore we initially chose λ constant.

The model equations (2.23) and (2.24) can then be written in dimensionless coordinates

$$\frac{\partial p}{\partial t} + |\nabla p|^2 = \frac{1}{N_1}(p - \phi) \tag{2.25a}$$

$$\frac{\partial \phi}{\partial t} + \nabla p \cdot \nabla \phi = (N_2 - \phi)\nabla^2 p \tag{2.25b}$$

where now the variables are dimensionless.

The model involves thus 2 dimensionless numbers:

$$N_1 = \frac{\lambda_0 \Delta p \tau}{L^2} \tag{2.26a}$$

$$N_2 = \frac{\gamma}{\Delta p} \tag{2.26b}$$

the first is a ratio between the time constant for gas mass transfer and a typical transport time and the second is a dimensionless (reciprocal) solubility. If the mobility would not be assumed constant, then the model would need a closure relation for the mobility function λ.

3 Solution methods

In order to validate the proposed approach we have chosen to perform comparisons between the proposed model, i.e. equations (2.23) and (2.24), and data from laboratory core flow experiments. It is supposed that the core length L is much larger than its diameter and that a one dimensional description in the axial co-ordinate x is sufficient (see figure 3.1).

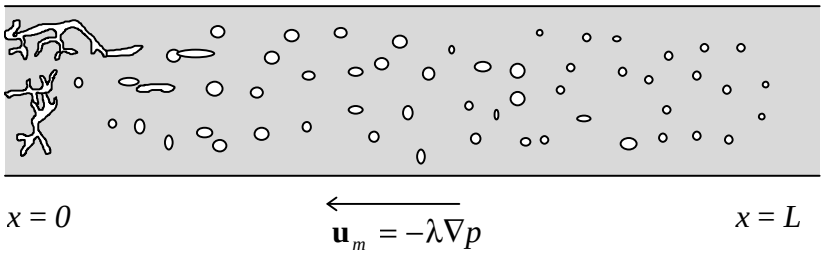

Figure 3.1 Schematic drawing of the de-pressurization of a core

A comparison with two types of core flow experiments is performed, which are both described by (2.23) and (2.24), but with different boundary conditions:

1. Core depressurization of a core closed at one end ($x = L$) and with given pressure at the other end ($x = 0$) (Sheng et al., 1996, Pooladi-Darvish & Firoozabadi, 1997, Firoozabadi, 1992, Huerta et al., 1996);
2. Core through flow with a given pressure gradient over the core (Maini & Sharma, 1994, Maini et al., 1993).

In numerical terms, these two cases correspond to the following boundary conditions:

1. one Neumann boundary condition $\partial p / \partial x\big|_{x=L} = 0$ and a Dirichlet boundary condition $p(0) = \tilde{p} - \Delta p(t)$
2. two Dirichlet boundary conditions: $p(L) = p_{sat}$, $p(0) = \tilde{p} - \Delta p$

Several solution strategies are possible, which will be discussed in the following.

3.1 Perturbation analysis

The equations (2.23) and (2.24) admit constant state solutions $p = p_0$ and $\phi = \phi_0$ which are solutions of the equilibrium solubility relation (2.15)

$$p_0 + \gamma\phi_0 = \tilde{p} \tag{3.1}$$

If we perturb these equilibrium solutions

$$p = p_0 + p' \tag{3.2a}$$

$$\phi = \phi_0 + \phi' \tag{3.2b}$$

and we neglect the terms which are quadratic in the perturbation variables, we obtain

$$\alpha\tau\frac{\partial p'}{\partial t} + p' + \gamma\phi' = 0 \tag{3.3a}$$

$$\alpha\frac{\partial \phi'}{\partial t} + (1-\phi_0)\lambda\nabla^2 p' = 0 \tag{3.3b}$$

where $\lambda = \lambda(\phi_0)$. The gradient cross term $\nabla\lambda \cdot \nabla p'$ has herein been neglected. We may eliminate p' or ϕ' from (3.3); in both cases we find a telegrapher's equation

$$\frac{\partial^2 p'}{\partial t^2} + \frac{1}{\alpha\tau}\frac{\partial p'}{\partial t} = c^2\nabla^2 p' \tag{3.4}$$

where

$$c = \left(\frac{(1-\phi_0)\lambda\gamma}{\tau\alpha^2}\right)^{1/2} \tag{3.5}$$

is a wave speed. The same equation is satisfied by ϕ'.

The waves are damped which is a result of the second term in (3.4). If the relaxation time $\tau \to 0$, then the effects of wave propagation gives way to diffusion

$$\frac{\partial p'}{\partial t} = \frac{(1-\phi_0)\lambda\gamma}{\alpha}\nabla^2 p' \tag{3.6}$$

Let us consider the solution of the telegraph equation (3.4) for "Stokes 1st problem" (see Joseph, 1990, pp. 582-584). The pressure p' at the boundary x = 0 of a semi-infinite region is suddenly raised and held at value Δp. We must solve (3.4) in one dimension

$$\frac{\partial^2 p'}{\partial t^2} + \frac{1}{\alpha\tau}\frac{\partial p'}{\partial t} = \frac{(1-\phi_0)\lambda\gamma}{\tau\alpha^2}\frac{\partial^2 p'}{\partial x^2} \tag{3.7}$$

satisfying the initial conditions

$$p'(x,t) = 0 \quad , t \le 0 \text{ and } x \ge 0 \tag{3.8}$$

and the boundary conditions

$$p'(0,t) = \Delta p H(t) \tag{3.9}$$

where $H(t)$ is Heaviside's step function, and

$$p'(x \to \infty, t) \to 0$$

Equation (3.7) can be written in a dimensionless form, using the wave speed (3.5), a length scale L, time scale $\alpha\tau$ and pressure scale Δp

$$\frac{\partial^2 p}{\partial t^2} + \frac{\partial p}{\partial t} = \left(\frac{c\alpha\tau}{L}\right)^2 \frac{\partial^2 p}{\partial x^2} \tag{3.10}$$

where now all variables are dimensionless.

Denoting

$$\hat{p}(s,t) = \mathcal{L}\left[p(x,t)\right] \tag{3.11}$$

and applying the Laplace transform $\mathcal{L}$ to (3.7)

$$\left(\frac{c\alpha\tau}{L}\right)^2 \frac{\partial^2 \hat{p}}{\partial x^2} = s(s+1)\hat{p} \tag{3.12}$$

which has solution

$$\left(\frac{c\alpha\tau}{L}\right)^2 \hat{p}(x,s) = \frac{1}{s}\exp\left[-\left\{s(1+s)\right\}^{1/2} x\right] \tag{3.13}$$

From inverse Laplace transform it is now found that the pressure as a function of space and time is given by

$$p(x,t) = \left(\frac{L}{c\alpha\tau}\right)^2 \mathcal{L}^{-1}\left(\frac{1}{s}\exp\left[-\left\{s(1+s)\right\}^{1/2} x\right]\right) \tag{3.14}$$

Analytical solution of (3.14) is difficult. Numerical evaluation of (3.14), using the technique of de Hoog et al (1982) can however easily be done by a readily available routine in the MATLAB programming language.

An important observation is that according to (3.4), the behavior of $\left(c\alpha\tau / L^2\right)p' / \Delta p$ as a function of x / L and $t / \alpha\tau$ is completely independent on the solubility constant and the transfer time τ. The form of the solutions stays thus always the same.

In some cases it is more convenient to choose the dimensionless time scale as $t\lambda\Delta p / \alpha L^2$. In dimensionless time, space gas fraction and pressure variables, the following equations is then found:

$$N_1 \frac{\partial^2 p}{\partial t^2} + \frac{\partial p}{\partial t} = \left(N_2 - \phi_0\right)\frac{\partial^2 p}{\partial x^2} \tag{3.10a}$$

with solution

$$p(x,t) = \mathcal{L}^{-1}\left(\frac{1}{s}\exp\left[-\left\{\frac{s(1+N_1 s)}{N_2 - \phi_0}\right\}^{1/2} x\right]\right) \tag{3.14}$$

For the case where nucleation is fast and $\tau \to 0$ ($N_1 \to 0$) it is straight forward to obtain an analytical solution by inverse Laplace transform

$$p = \text{erfc}\left[\frac{1}{\left(N_2 - \phi_0\right)^{1/2}}\frac{x}{2\sqrt{t}}\right] \tag{x.18}$$

In this case thus similarity solutions exist in the variable $\zeta = x / \sqrt{t}$.

3.2 Steady state solution

A steady state solution is of interest in the open core problem, where a gradient in gas fraction and pressure are set up. The one-dimensional steady state equations obtained from (2.23) and (2.24) are

$$-\lambda\left(\frac{dp}{dx}\right)^2 = \frac{\tilde{p} - p - \gamma\phi}{\tau} \tag{3.15}$$

$$\frac{d}{dx}\left\{(1-\phi)\left(-\lambda\frac{dp}{dx}\right)\right\} = 0 \tag{3.16}$$

The second equation integrates to

$$\frac{dp}{dx} = -\frac{u_0}{\lambda(1-\phi)} \tag{3.17}$$

where u_0 is a integration constant of dimension velocity.

A second integration gives

$$\tilde{p} - p = \int_0^x \frac{u_0}{\lambda(1-\phi)}dx \tag{3.18}$$

Substituting (3.17) and (3.18) in (3.15) we obtain

$$\gamma\phi - \frac{\tau u_0^2}{\lambda(1-\phi)^2} = \int_0^x \frac{u_0}{\lambda(1-\phi)}dx \tag{3.19}$$

which differentiates to

$$\left\{\gamma - \frac{2\tau u_0^2}{\lambda(1-\phi)^3}\right\}\frac{d\phi}{dx} = \frac{u_0}{\lambda(1-\phi)} \tag{3.20}$$

This can be integrated between an arbitrary position in the core and the end $x = L$ where the pressure is the saturation pressure and the gas fraction equal to zero

$$\int_\phi^0 \left\{(1-\phi) - \frac{2\tau u_0^2}{\lambda\gamma}(1-\phi)^{-2}\right\}d(1-\phi) = -\int_x^L \frac{u_0 dx}{\lambda\gamma} \tag{3.20a}$$

The result is

$$(1-\phi)^3 - \left\{1 - \frac{4\tau u_0^2}{\lambda\gamma} + \frac{2u_0 L}{\lambda\gamma}\left(1 - \frac{x}{L}\right)\right\}(1-\phi) - \frac{4\tau u_0^2}{\lambda\gamma} = 0 \tag{3.20c}$$

Using a dimensionless gas fraction $\phi\gamma / \Delta p$, a dimensionless length x / L and a dimensionless integration constant $u_0 L / \lambda\Delta p$ (in the following ϕ, x and u_0 are thus dimensionless variables

$$\left(1-\frac{\Delta p\phi}{\gamma}\right)^3-\left\{1-4N_1N_2u_0^2+2u_0(1-x)\right\}\left(1-\frac{\Delta p\phi}{\gamma}\right)-4N_1N_2u_0^2=0 \qquad (3.20c)$$

The dimensionless numbers N_1 and N_2 are defined in (2.26). This third order polynomial has an analytical solution.

3.3 Equilibrium solution

If the gas can come out of solution infinitely fast, then $\tau=0$ and the equilibrium solubility (2.15) replaces the constitutive equation (2.16). Equation (2.15) states that the gas fraction is high where the pressure is low. The bubbles and the oil flow from regions with higher pressure to regions with lower pressure and thus to regions with higher gas fraction. From (2.15) the gas fraction can be expressed in the pressure as

$$\phi=\frac{\tilde{p}-p}{\gamma} \qquad (3.23)$$

Substituting this expression in (2.24) a non-linear diffusion equation is obtained

$$-\alpha\frac{\partial p}{\partial t}+\lambda|\nabla p|^2=(\gamma+p-\tilde{p})\nabla\cdot(-\lambda\nabla p) \qquad (3.24)$$

Prof. G.I. Barenblatt has noted that (3.24) can be rearranged in

$$\alpha\frac{\partial p}{\partial t}=\nabla\cdot\left(D(p)\nabla p\right) \qquad (3.25)$$

with diffusion coefficient

$$D(p)=\lambda(\gamma+p-\tilde{p}) \qquad (3.26)$$

If we define

$$\hat{p}:=\gamma+p-\tilde{p} \qquad (3.27a)$$

$$\psi:=\int_{\hat{p}}\lambda(x)\hat{p}d\hat{p} \qquad (3.27b)$$

then (3.25) can be written as

$$\alpha\frac{\partial\hat{p}}{\partial t}=\nabla^2\psi \qquad (3.28)$$

which for constant λ simplifies to the well-known Boussinesq equation (Kalashnikov, 1987)

$$\alpha\frac{\partial\hat{p}}{\partial t}=\frac{\lambda}{2}\nabla^2\hat{p}^2 \qquad (3.29)$$

In order to solve the one-dimensional equilibrium equation numerically it is convenient to write the equations in dimensionless co-ordinates. Therefore we use the dimensionless pressure $(\tilde{p}-p)/\Delta p$ and time $t\lambda\Delta p/\alpha L$. The length scale is made dimensionless by the core length L.

$$\frac{\partial p}{\partial t}=\frac{d}{dx}\left((N_2-p)\frac{dp}{dx}\right) \qquad (3.30)$$

Equation (3.30) can be written as

$$\frac{\partial p}{\partial t}=\frac{\partial^2 z}{\partial x^2} \qquad (3.30)$$

with

$$z = N_2 p - p^2 / 2 \tag{3.31}$$

The time and the domain are discretized by

$$t = (n-1)\Delta t, \quad 1 \le n \le N \tag{3.32a}$$

$$x = (j-1)\Delta x, \quad 1 \le j \le J \tag{3.32b}$$

with

$$\Delta t = t_{\max} / (N-1) \tag{3.33a}$$

$$\Delta x = 1 / (J-1) \tag{3.33b}$$

Using an implicit Cranck-Nicholson scheme, (3.30) writes

$$\frac{p_j^{n+1} - p_j^n}{\Delta t} = 0.5 \frac{z_{j-1}^{n+1} - 2z_j^{n+1} + z_{j+1}^{n+1}}{\Delta x^2} + 0.5 \frac{z_{j-1}^n - 2z_j^n + z_{j+1}^n}{\Delta x^2} \tag{3.34}$$

Each (n+1) term on the right hand side of (3.34) can be linearized by

$$z_*^{n+1} = z_*^n + \left(p_*^{n+1} - p_*^n\right) \left.\frac{\partial z}{\partial p}\right|_{*,n} = z_*^n + \left(p_*^{n+1} - p_*^n\right) D_*^n \tag{3.35}$$

where * indicates (j-1, j, j+1), resulting in

$$\begin{aligned} &\frac{p_j^{n+1}}{\Delta t} - 0.5 \frac{D_{j-1}^n p_{j-1}^{n+1} - 2D_j^n p_j^{n+1} + D_{j+1}^n p_{j+1}^{n+1}}{\Delta x^2} = \\ &\frac{p_j^n}{\Delta t} - 0.5 \frac{D_{j-1}^n p_{j-1}^n - 2D_j^n p_j^n + D_{j+1}^n p_{j+1}^n}{\Delta x^2} + \frac{z_{j-1}^n - 2z_j^n + z_{j+1}^n}{\Delta x^2} \end{aligned} \tag{3.36}$$

where

$$D_j^n = N_2 - p_j^n \tag{3.37}$$

Noting

$$s = \frac{\Delta t}{\Delta x^2} \tag{3.38}$$

equation (3.36) becomes

$$\begin{aligned} &-0.5sD_{j-1}^n p_{j-1}^{n+1} + \left(1 + sD_j^n\right) p_j^{n+1} - 0.5sD_{j+1}^n p_{j+1}^{n+1} = sz_{j-1}^n - 2sz_j^n + sz_{j+1}^n \\ &-0.5sD_{j-1}^n p_{j-1}^n + \left(1 + sD_j^n\right) p_j^n - 0.5sD_{j+1}^n p_{j+1}^n \end{aligned} \tag{3.39}$$

The values of z_j^n is given by (3.31) as

$$z_j^n = N_2 p_j^n - p_j^{n^2} / 2 \tag{4.40}$$

The boundary condition at j = J (x = 1) can either be Neumann, in which case we discretize it as

$$\frac{p_{J+1}^n - p_{J-1}^n}{\Delta x} = 0 \tag{3.42}$$

and then

$$\begin{aligned} &-sD_{J-1}^n p_{J-1}^{n+1} + \left(1 + sD_J^n\right) p_J^{n+1} = 2sz_{J-1}^n - 2sz_J^n \\ &-sD_{J-1}^n p_{J-1}^n + \left(1 + sD_J^n\right) p_J^n \end{aligned} \tag{3.41b}$$

or Dirichlet ($p_J = 0$) in which case

$$\left(1+sD_{J-1}^{n}\right)p_{J-1}^{n+1}-0.5sD_{J-2}^{n}p_{J-2}^{n+1}=-2sz_{J-1}^{n}+sz_{J-2}^{n}+$$
$$\left(1+sD_{J-1}^{n}\right)p_{J-1}^{n}-0.5sD_{J-2}^{n}p_{J-2}^{n} \qquad (3.41a)$$

The boundary condition at $j = 1$ ($x = 0$) is always a Dirichlet boundary condition so that for $j = 2$, equation (3.39) becomes

$$\left(1+sD_{2}^{n}\right)p_{2}^{n+1}-0.5sD_{3}^{n}p_{3}^{n+1}=sz_{3}^{n}-2sz_{2}^{n}+sz_{1}^{n}$$
$$\left(1+sD_{2}^{n}\right)p_{2}^{n}-0.5sD_{3}^{n}p_{3}^{n}+0.5s\left(D_{1}^{n}p_{1}^{n+1}-D_{1}^{n}p_{1}^{n}\right) \qquad (3.43)$$

Equation (3.39) can be written in a matrix representation

$$\mathbf{A}\mathbf{p}^{n+1}=\mathbf{A}\mathbf{p}^{n}+\mathbf{d}^{n} \qquad (3.44)$$

The closed core problem is defined by (3.36), (3.41*a*) and (3.43) and yields

$$\mathbf{A}=\begin{bmatrix} 1+s\left(N_2-p_2^n\right) & -0.5s\left(N_2-p_3^n\right) & & & \\ -0.5s\left(N_2-p_3^n\right) & 1+s\left(N_2-p_4^n\right) & -0.5s\left(N_2-p_5^n\right) & & \\ & \ddots & \ddots & & \\ & -0.5s\left(N_2-p_{j-1}^n\right) & 1+s\left(N_2-p_j^n\right) & -0.5s\left(N_2-p_{j+1}^n\right) & \\ & & \ddots & & \\ & & -s\left(N_2-p_{J-1}^n\right) & 1+s\left(N_2-p_J^n\right) & \end{bmatrix} \qquad (3.45a)$$

$$\mathbf{p}^{n}=\begin{bmatrix} p_2^n & \cdots & p_J^n \end{bmatrix}^T \qquad (3.45b)$$

$$\mathbf{d}^{n}=\begin{bmatrix} sz_1^n-2sz_2^n+sz_3^n+0.5s\left(D_1^n p_1^{n+1}-D_1^n p_1^n\right) \\ sz_2^n-2sz_3^n+sz_4^n \\ \vdots \\ sz_{j-1}^n-2sz_j^n+sz_{j+1}^n \\ \vdots \\ 2sz_{J-1}^n-2sz_J^n \end{bmatrix} \qquad (3.45c)$$

The open core with prescribed pressure drop, given by (3.36), (3.41*a*) and (3.43) leads to

$$\mathbf{A}_1 = \begin{bmatrix} 1+s\left(N_2 - p_2^n\right) & -0.5s\left(N_2 - p_3^n\right) & & & \\ -0.5s\left(\gamma - p_3^n\right) & 1+s\left(N_2 - p_4^n\right) & -0.5s\left(N_2 - p_5^n\right) & & \\ & \ddots & \ddots & & \\ & -0.5s\left(N_2 - p_{j-1}^n\right) & 1+s\left(N_2 - p_j^n\right) & -0.5s\left(N_2 - p_{j+1}^n\right) & \\ & & \ddots & & \\ & & -0.5s\left(N_2 - p_{J-2}^n\right) & 1+s\left(N_2 - p_{J-1}^n\right) & \end{bmatrix} \tag{3.46a}$$

$$\mathbf{p}^n = \begin{bmatrix} p_2^n & \cdots & p_{J-1}^n \end{bmatrix}^T \tag{3.46b}$$

$$\mathbf{d}^n = \begin{bmatrix} sz_1^n - 2sz_2^n + sz_3^n + 0.5s\left(D_1^n p_1^{n+1} - D_1^n p_1^n\right) \\ sz_2^n - 2sz_3^n + sz_4^n \\ \vdots \\ sz_{j-1}^n - 2sz_j^n + sz_{j+1}^n \\ \vdots \\ sz_{J-2}^n - 2sz_{J-1}^n + sz_J^n \end{bmatrix} \tag{3.46c}$$

3.4 Full numerical solution

... all this work still has to be done....

4 Results

4.1 Depressurization of a closed core

The result of the equilibrium solution are shown in figure 4.1 and 4.2 for N_2 values of 2 and 20. The main influence of increasing N_2, which corresponds to increasing γ or lowering the solubility is a faster propagation of the pressure drop into the core. This is in agreement with the perturbation analysis where a wave speed is found which is proportional to $\gamma^{1/2}$.

In figure 4.3 and 4.4 we compare the same cases, but evaluated with the perturbation analysis, leading to the telegrapher's equation. In the case of a very small time constant of transfer, the telegraph equation degenerates into a diffusion equation with solutions which take the form of complementary error function (see equation x.18).

At small time the results of the perturbation analysis and of the numerical solution are identical. At large time however, the perturbation analysis results do not approach the new equilibrium situation as fast as predicted by the numerical solution.

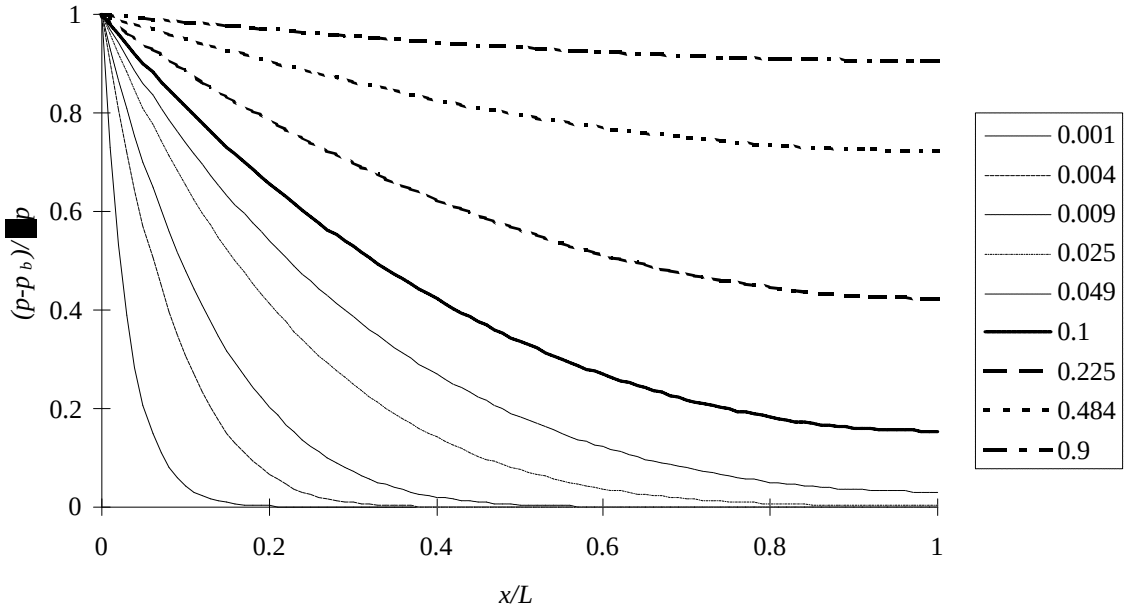

Figure 4.1 Closed core depressurization problem: equilibrium solution for N_2 = 2 in dimensionless co-ordinates; pressure as a function of space at different times. pb *indicates the bubbles point pressure* $\tilde{p}$.

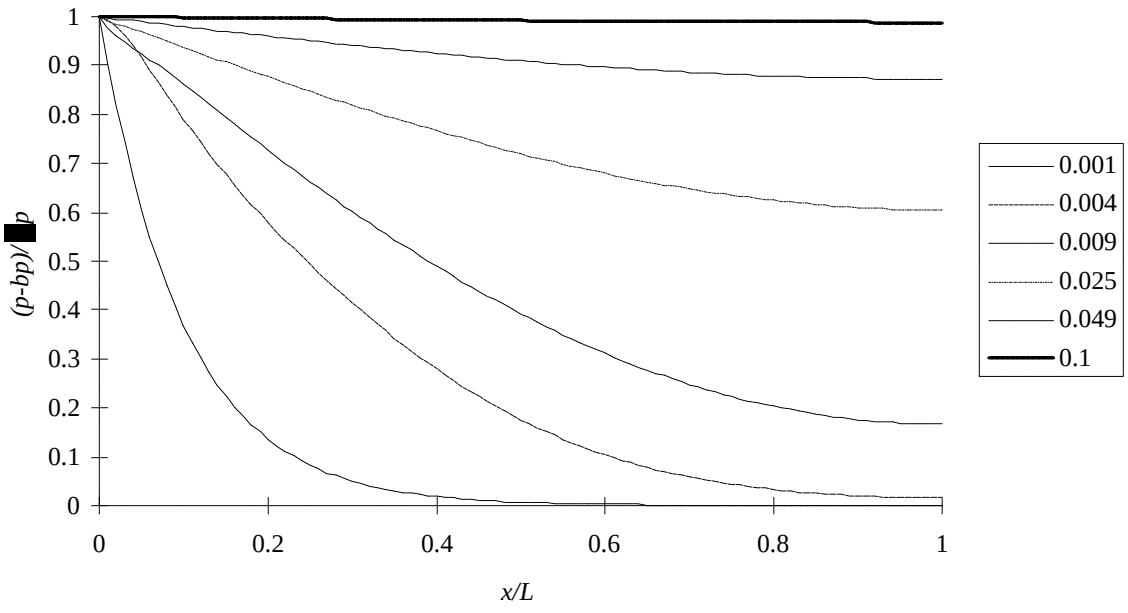

Figure 4.2 Closed core depressurization problem: equilibrium solution for N_2 = 20 in dimensionless co-ordinates; pressure as a function of space at different times. pb *indicates the bubbles point pressure* $\tilde{p}$.

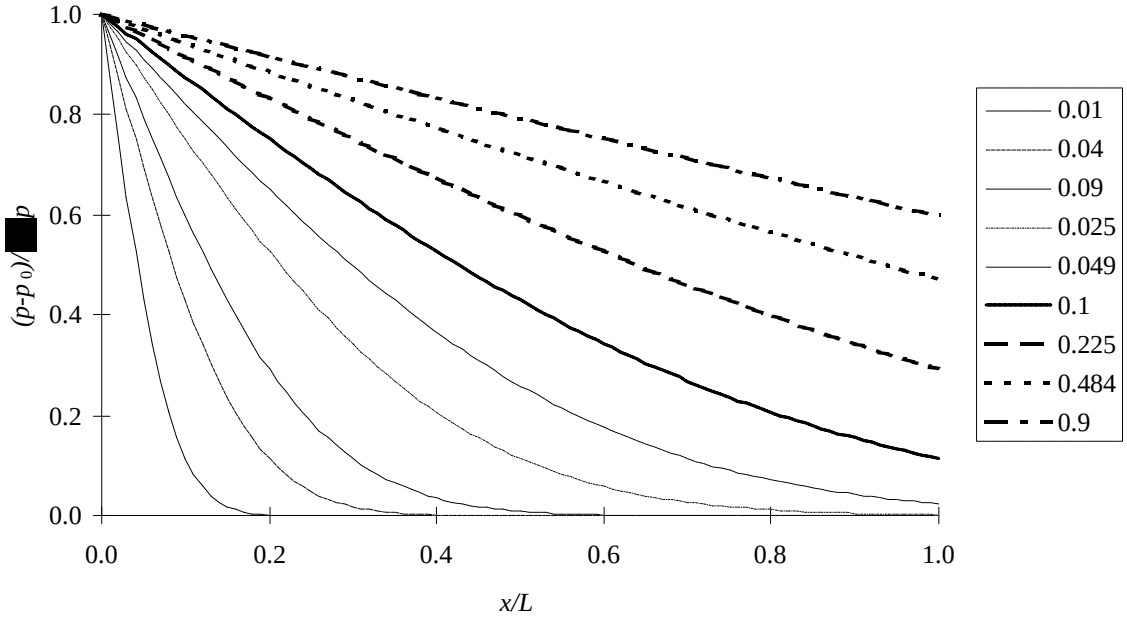

Figure 4.3 Closed core depressurization problem: equilibrium solution with perturbation analysis for N_2 = 2 in dimensionless co-ordinates; pressure as a function of space at different times. p_0 *indicates the pressure which satisfies the constant state solutions.*

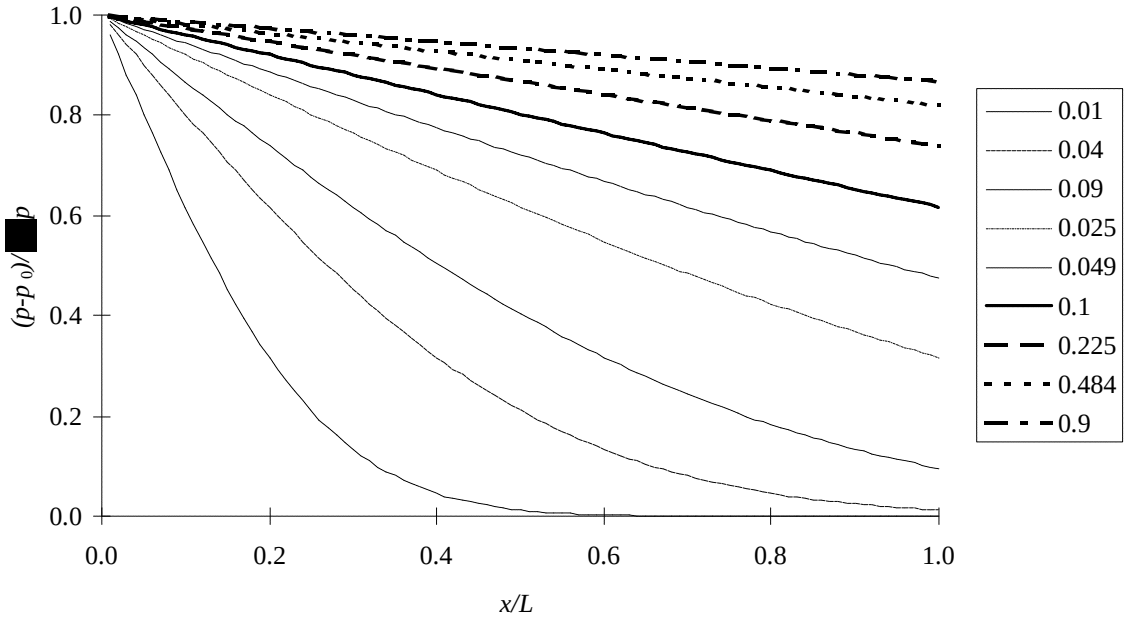

Figure 4.4 Closed core depressurization problem: equilibrium solution with perturbation analysis for N_2 = 20 in dimensionless co-ordinates; pressure as a function of space at different times. p_0 *indicates the pressure which satisfies the constant state solutions.*

The result of increasing the transfer time is shown in figures 4.5 and 4.6 for $N_2 = 2$. A propagating discontinuity in the space derivative of pressure is found, which becomes more pronounced as the time scale is increased.

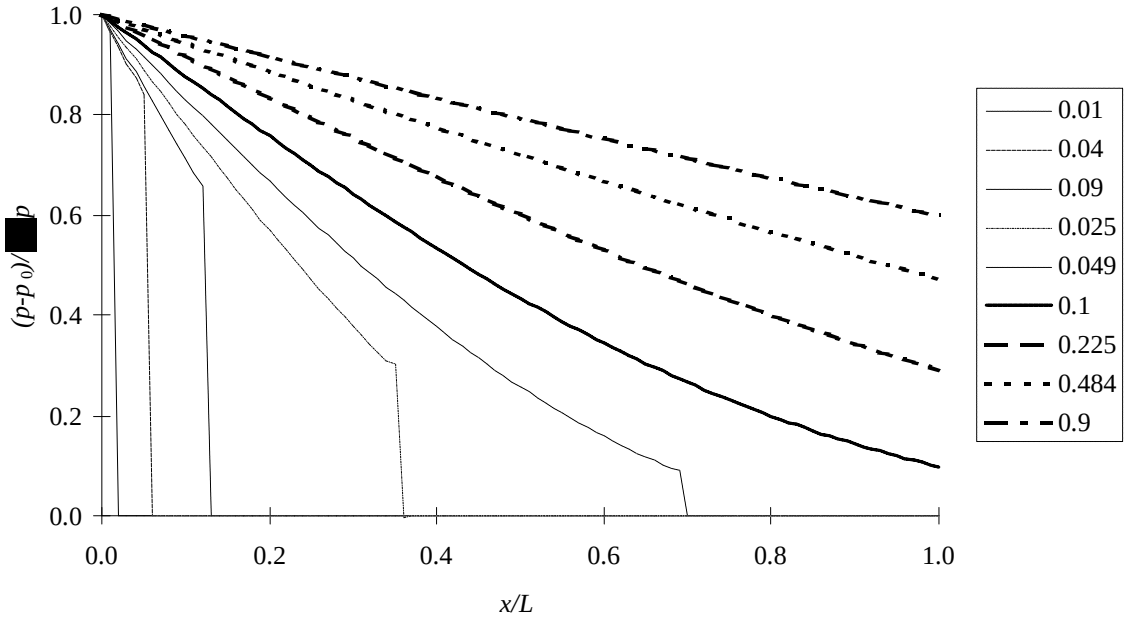

Figure 4.5 Closed core depressurization problem: equilibrium solution with perturbation analysis for $N_2 = 2$ and N_1=0.01 *in dimensionless co-ordinates; pressure as a function of space at different times.* p_0 *indicates the pressure which satisfies the constant state solutions.*

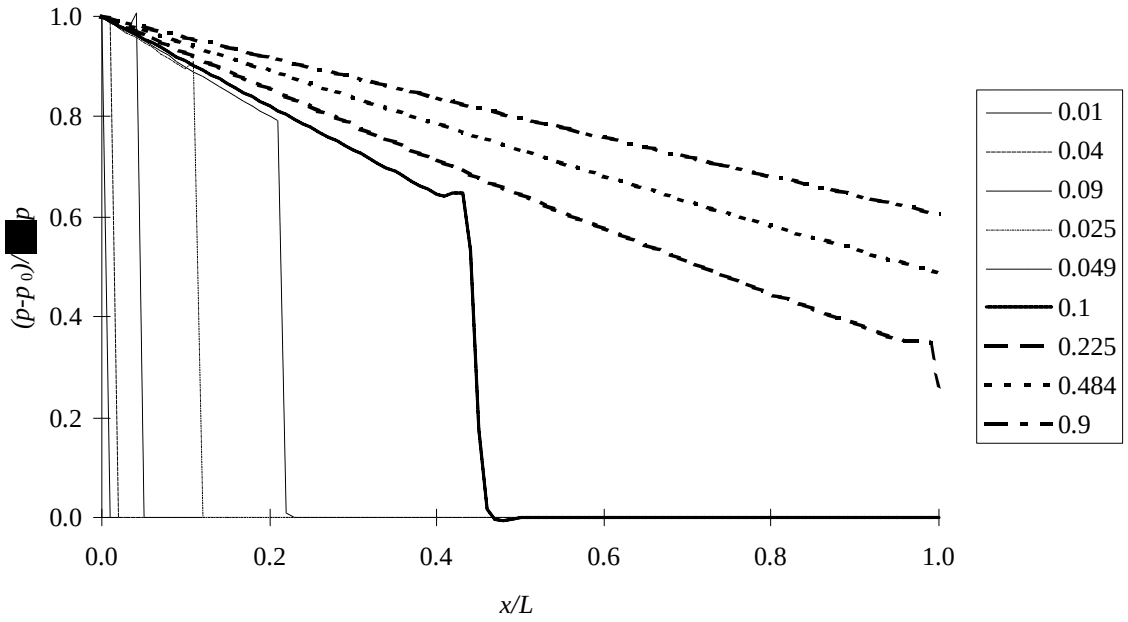

Figure 4.6 Closed core depressurization problem: equilibrium solution with perturbation analysis for N_2 = 2 and N_1=0.1 *in dimensionless co-ordinates; pressure as a function of space at different times.* p_0 *indicates the pressure which satisfies the constant state solutions.*

When rendered dimensionless by a time scale $\alpha\tau$ as was done for equation (3.14), the solutions of the perturbation equations in the dimensionless co-ordinates $p^* = (p/\Delta p)(L/c\alpha\tau)^2$ and $x^* = x/L$ do not depend on any parameters other than those embedded in the non-dimensionalization. The solution of (3.14) is shown in figure 4.7.

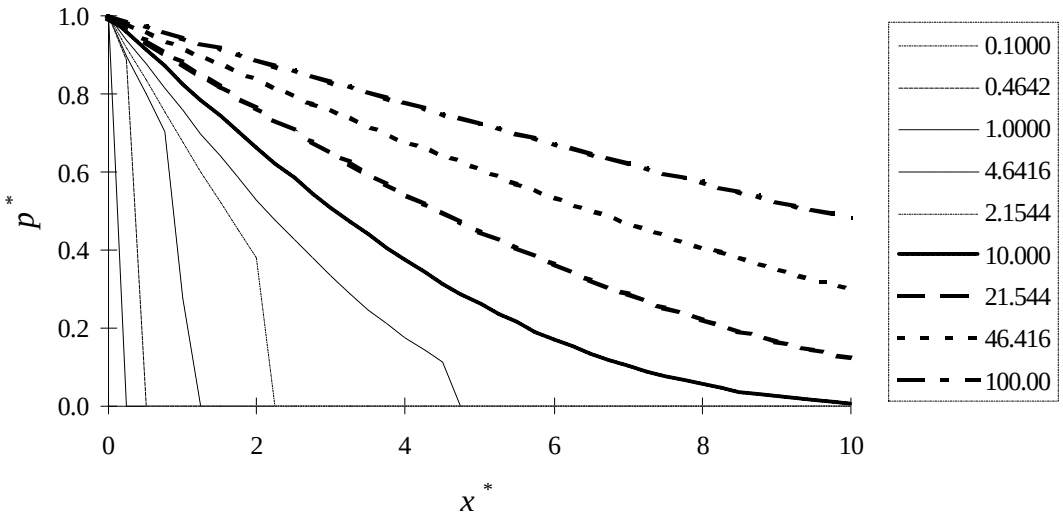

Figure 4.7 Numerical evaluation of equation (3.14): pressure versus distance in the core at different times; a discontinuity in the derivative propagates into the core

The pressure disturbance propagates into the core, resulting in a discontinuity in the space derivative of the pressure which propagates at a speed c and an attenuation given by

$$p'(x, x/c) = p_0' \exp\left(\frac{\alpha\tau x}{2c}\right) \tag{4.1}$$

If the result is plotted versus a similarity co-ordinate $\varsigma = (\alpha\tau)^{1/2} L^{-1} x / \sqrt{t}$, we observe that at large times a similarity solution can be found.

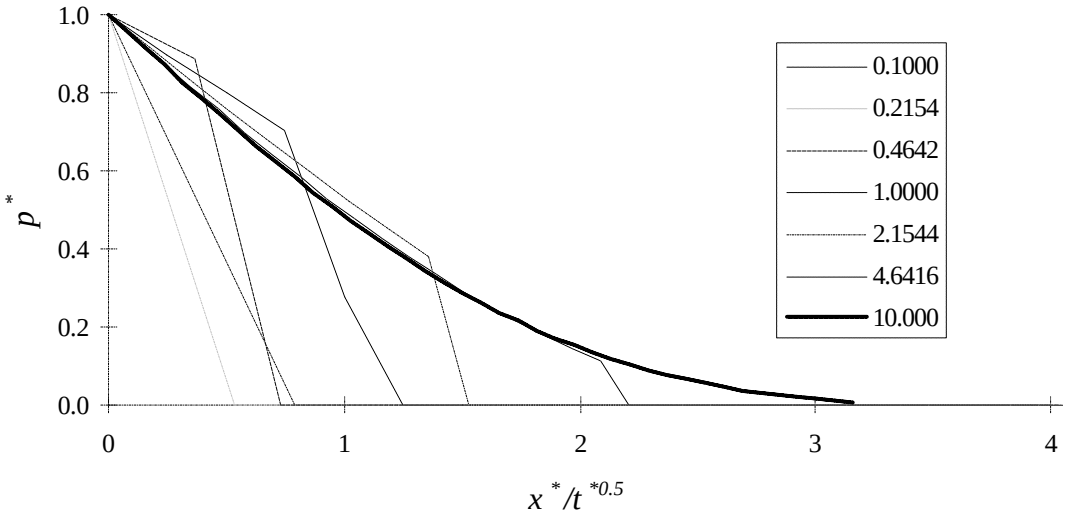

Figure 4.8 Numerical evaluation of equation (3.14): pressure versus similarity co-ordinate $x^* / \sqrt{t^*}$ at different times; at large times a similarity solution can be observed

4.2 Flow in an open core with imposed pressure drop

5 Conclusions

Acknowledgments: Prof. G.I. Barenblatt (University of California) is acknowledged for some useful comments.

6 Appendix A: an alternative form of the constitutive equation

A general constitutive law of type

$$a\frac{D\phi}{Dt}+b\frac{Dp}{Dt}=f(p,\phi) \tag{A.1}$$

has been assumed in section 2.2, where the special case $a = 0$ has been investigated in detail. If we choose $b = 0$, equation (A.1) can be written as

$$\tau\gamma\frac{D\phi}{Dt}+\gamma\phi=\tilde{p}-p \tag{A.2}$$

which is a statement that the volume fraction relaxes toward the equilibrium value, with time constant τ. Using definition (2.3) of the material derivative in (A.2) yields

$$\tau\gamma\frac{\partial\phi}{\partial t}-\tau\gamma\lambda\nabla p\cdot\nabla\phi+\gamma\phi=\tilde{p}-p \tag{A.2}$$

Equations (A.2) and (2.24) are the basic governing equations in this form of the theory. Clearly, when τ = 0, we recovery exactly the same equilibrium theory as was derived above. It is also clear that this version of the theory supports steady uniform states as solution, again exactly as found above. The governing equations for small perturbations around these steady states are however different, as we shall now show. As before, introduce small perturbation quantities defined by (3.2) where equilibrium demands that (3.1) holds. Substituting these quantities into (A.2) and (2.24), neglecting quantities of second order in perturbations and treating the mobility as a constant, we obtain

$$\alpha\tau\gamma\frac{\partial\phi'}{\partial t}+\gamma\phi'=-p' \tag{A.3}$$

$$\alpha\frac{\partial\phi'}{\partial t}+(1-\phi_0)\lambda\nabla^2p'=0 \tag{A.4}$$

where $\lambda=\lambda(\phi_0)$. If we now take the time derivative of (A.3), and use (A.4) to replace $\partial\phi'/\partial t$ by the Laplacian of p', we find

$$\alpha\left\{1-\tau(1-\phi_0)\lambda\gamma\nabla^2\right\}\frac{\partial p'}{\partial t}=(1-\phi_0)\lambda\gamma\nabla^2p' \tag{A.5}$$

The perturbation volume fraction satisfies an identical equation. Initial and boundary conditions on the perturbation pressure are the same here as for the model presented above.

The evolution equation for the perturbation pressure, (A.5), is very different in character from the telegraph equation found for the pressure relaxation form of the constitutive law. It is lower order in time, and, from Laplace transform solutions, appears not to exhibit wave propagation; rather, the solutions are diffusive in character although similarity solutions in $x/t^{1/2}$ do not exist (except as an asymptotic state at large *t*). The

rate of advance of the pressure perturbation front is found from these Laplace transform solutions to be faster in early time than would be the case for classical diffusion.

7 References

Chesters, A.K., 1991, "The modelling of coalescence processes in fluid-liquid dispersion: a review of current understanding", Trans. I. Chem. Engng., **69**(part A):259-270.

Denbigh K., 1981, "The principles of chemical equilibrium", Cambridge University Press.

Firoozabadi A., Ottensen B., Mikkelsen M., 1992, "Measurements of super saturation and critical gas saturation", SPE Formation Evaluation, December, pp. 337-344.

Geilikman M.B., Dusseault M.B., Dullien F.A.L., 1995, "Dynamic effects of foamy fluid flow in sand production instability" International Heavy Oil Symposium, Calgary, Alberta, Canada, 19-21 June 1995, SPE 30251.

de Hoog et al., 1982, "...", SIAM J. Sci. Stat. Comput., **3**(3):357-366.

Huerta M, Otero C., Jiménez I., de Mirabel M., Rojas G., 1996, Understanding foamy oil mechanisms for heavy oil reservoirs during primary production, SPE Annual Technical Conference and Exhibition, Denver, Colorado, USA, 6-9 October 1996, SPE 36749.

Joseph D.D., 1997, "Foamy oil flow in a porous media", memo for Intevep S.A., department EPYC, dated September 16.

Joseph D.D., 1990, "Fluid dynamics of viscoelastic liquids", Springer Verlag. *Appl. Math Sciences*, **84**.

Kalashnikov E.S., 1987, "Some problems of the qualitative theory of non-linear degenerate second order parabolic equations", Russian Mathematical Surveys, **42**(2):169-222.

Maini B.B., Sharma H.K., 1994, "Role of nonpolar foams in production of heavy oils", in: Foams: fundamentals & Applications in the Petroleum Industry, Advances in Chemistry Series, **242**: 405-420.

Maini B.B., Sharma H.K, George A.E., 1993, "Significance of foamy-oil behavior in primary production of heavy oil", J. Canad. Petr. Tech., **32**(9):50-54.

Maini B.B., 1996, "Foamy oil flow in heavy oil production", J. Can. Petrol. Tech., **35**(6): 21-22,24.

Pooladi-Darvish M., Firoozabadi A., 1997, "Solution gas drive in heavy oil reservoirs", 48th Annual Technical Meeting of the Petroleum Society of the SIM, Calgary, Canada, June 11, SIM, paper 97-113, 13 pp.

Reamer H.H., Olds R.H., Sage B.H., Lacey W.N., 1942, "Phase equilibria in hydrocarbon systems", Ind. & Eng. Chem., 34(12):1526-1531.

Sheng J.J., Hayes R.E., Maini B.B., Tortike W.S., 1995, "A proposed dynamic model for foamy oil properties", International Heavy Oil Symposium, Calgary, Alberta, Canada, 19-21 June, SPE 30253.

Sheng J.J., Hayes R.E., Maini B.B., Tortike W.S., 1996, "A dynamic model to simulate foamy oil flow in porous media", 1996 SPE Annual Technical Conference and Exhibition, Denver, Colorado, USA, 6-9 October, SPE 36750.

Smith G.E., "Fluid flow and sand production in heavy oil reservoirs under solution gas drive, 56th California regional meeting of the SPE, Oakland, CA., April 2-4, SPE 15094.

Svrcek W.Y., Mehrotra A.K., 1982, "Gas solubility, viscosity and density measurements for Athabasca bitumen", *J. Canadian Petroleum Technology*, **21** (4): 31-38.

Wang Y., 1997, "Sand production and foamy oil flow in heavy-oil reservoirs", SPE International Thermal Operations and Heavy Oil Symposium, Bakersfield, CA, Feb. 10-12, SPE 37553.